arXiv:1704.03588v2 [cond-mat.stat-mech] 13 Apr 2017

Ensemble Inequivalence and Maxwell Construction in the Self-Gravitating Ring Model

T. M. Rocha Filho* and M. A. Amato

Instituto de Física and International Center for Condensed Matter Physics, Universidade de Brasília, CP 04455, 70919-970 - Brasília, Brazil

C. H. Silvestre

Instituto de Física, Universidade de Brasília, CP 04455, 70919-970 - Brasília, Brazil

Abstract

Equilibrium Statistical Mechanics is undoubtedly a cornerstone for the description of many particle systems. The common interpretation is based on ensemble theory as put forward by Gibbs, alongside the basic assumptions that different ensembles are equivalent, i. e. the properties of the system can equally be obtained in any ensemble with the same results. However, the simplicity of the argument that provides such equivalence, mathematically grounded by the existence of Legendre transformation between the ensembles and the existence of its inverse, may break down for physical systems with long range interactions. In this paper we study the behavior of a simple toy model with a long range interaction and show from first principles, by solving numerically the mechanical equations of motion and Monte Carlo simulations, the inequivalence of ensembles, and discuss in what situations and how the Maxwell construction is applicable.

PACS numbers: 05.10.Gg, 05.20.-y, 05.20.Dd

* marciano@fis.unb.br

I. INTRODUCTION

Equilibrium Statistical Mechanics is a hallmark of theoretical physics and an invaluable tool to study the properties of matter for more than a century. At its foundations lie Gibbs' ensembles theory [1], which is an elegant formulation applicable to a very broad class of phenomena (for a brief history of ensemble theory see [2]). As it is well known for any rounded practitioner, the microcanonical ensemble is harder to use than the canonical ensemble, and the grandcanonical ensemble is in a sense still simpler than the canonical one. Provided that the predictions of different ensembles coincide, one can then choose which one to use according to the needs in consideration. As a consequence, many authors devoted a considerable effort to the task of proving and establishing the limits of validity of the equivalence of the different ensembles (see [3] and references therein). From the thermodynamical viewpoint ensemble equivalence is based on the fact that the Legendre transformation connecting different ensembles is invertible. This implies particularly that the entropy is a concave function of the energy in the whole physically accessible energy range. In statistical terms it means that all properties of the system are well described either in terms of energy or temperature, that is the essentially Gibbs' argument. On the other hand, it also follows that the appearance of a convexity region in the entropy-energy curve breaks down the equivalence. In this case any state of the system in the convex region cannot be realized in the canonical ensemble and the simplicity of Gibbs argument fails. A rigorous mathematical proof of such results are given in Ref. [4].

For the aim of the present work we limit ourselves here to classical many particle systems composed of N identical particles in d spatial dimensions, with Hamiltonian

$$H = \sum_{i=1}^{2} \frac{p_i^2}{2m} + U^{(N)}(\mathbf{r}_1, \dots \mathbf{r}_N), \tag{1}$$

with $U^{(N)}$ being the potential energy depending on particle positions $\mathbf{r}_i$, $i = 1, \dots, N$ and $\mathbf{p}_i$ their conjugate momenta. In Ref. [5] the following definitions are introduced:

Definition I.1. Tempered interaction: an interaction potential is said tempered if there exists $\lambda > d$, $R_0 > 0$ and $A \geq 0$ such that $W_{\text{int}}(\mathbf{r}_1, \dots \mathbf{r}_N) = U^{(N)}(\mathbf{r}_1, \dots \mathbf{r}_N) - U^{(N_1)}(\mathbf{r}'_1, \dots \mathbf{r}'_{N_1}) - U^{(N_2)}(\mathbf{r}''_1, \dots \mathbf{r}''_{N_2}) \leq AN_1N_2/r^\lambda$, whenever $|\mathbf{r}'_i - \mathbf{r}''_j| \geq r \geq R_0$, for $i = 1, \dots N_1$ and $j = 1, \dots N_2$.

Definition I.2. Stable interaction: an interaction potential is stable if there exists a constant $B \geq 0$ such that $U^{(N)}(\mathbf{r}_1, \ldots \mathbf{r}_N) \geq -NB$, for all values of N.

It was then proved that the microcanonical, canonical and grandcanonical ensembles for a system with Hamiltonian in Eq. (1) are equivalent in the thermodynamic limit $N \to \infty$ if the interaction potential is tempered and stable. The Helmholtz free energy and the grand-potential are obtained from the microcanonical entropy and the usual Legendre transforms.

Definition I.1 essentially ensures that energy is additive, and definition I.2 that a stable equilibrium state exists. Examples of physically relevant and non-stable potentials are the gravitational interaction, where the non-stability leads to the so-called gravothermal catastrophe [6], and multi-species plasmas [5].

A special case must be discussed now, when a first-order phase transition occurs in the system. In this case the entropy can be schematically represented as in Fig. 1, where a convex intruder may exist for finite N, and is depicted in the figure in the energy interval between point A and B, these two points corresponding to two different phases. Regions I and III correspond to metastable states and region II to unstable states with a negative heat capacity. In the latter case the states are strictly unstable as a small fluctuation in the temperature causes a runaway effect. On the other hand, according to van Hove's theorem [7], and under certain assumptions, the pressure P in the canonical ensemble must be a decreasing function of the volume V and become constant for the values of V in the interval of phase coexistence (the volume interval for energies E_A to E_B). In the microcanonical ensemble this corresponds to the straight line connecting points A and B in Fig. 1. In the canonical ensemble this implies that no van der Waals loop exist in the free energy (see below) and that the convex intruder disappears in the thermodynamic limit and is replaced by the this same straight line. This is the Maxwell construction prescription.

One of the conditions required in van Hove's theorem is that, for a three-dimensional system, the interparticle potential $V(r)$ satisfies $V(r) \geq r^{-3-\alpha}$ for $\alpha > 0$ and large distances r, i. e. that the potential is short-ranged and the total energy is additive. Therefore, in equilibrium statistical mechanics calculations, a convex intruder in the entropy function can only exist as a result of approximations, e. g. using a mean-field approach for a system with short-range interactions, or because the size of the system is not sufficiently large [8–10]. This point is very well illustrated for the two-dimensional Potts model with nearest neighbors interaction, where a convex dip is present for small lattice size, disappearing for increasing

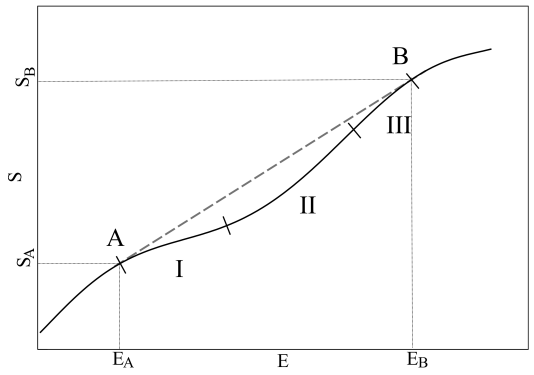

FIG. 1.

N with the negative specific region being replaced by a flat curve (i. e. the straight line in Fig. 1). On the other hand for globally coupled spins, the convex dip remains even in the thermodynamic limit [12].

As already discussed above, the usual prescription to deal with a convex dip in the entropy is the Maxwell construction. It replaces the convex region in the entropy by a straight line shown in Fig. 1 that describes the coexistence of two phases A and B, and given by $S = S_A(1-a) + S_B\, a$, $0 \leq a \leq 1$, where a is the fraction of the system in phase A and $1-a$ the fraction in phase B. The resulting entropy is then the sum of the entropies in each phase. The additivity of the energy, and consequently also of the entropy, is guaranteed by the temperedness of the potential energy, and the relevant thermodynamic potential in the canonical ensemble is the free energy obtained as the Legendre transform of the entropy. If the entropy is not strictly concave, the inverse Legendre transform of the free energy differs from the original microcanonical entropy and there is information loss when passing from the microcanonical to the canonical ensemble [13].

The additivity of energy and entropy, which follows from the temperedness of the potential, and its stability, ensure that equilibrium ensembles are equivalent. The important point is that there exist real systems for which these conditions are not met. This does not imply that ensembles are not equivalent as the conditions are sufficient but not necessary. On the other hand, there are systems for which ensembles are inequivalent. One could cite as an example a system of self-gravitating particles in 3D, as from the virial theorem we have for the total energy of a stationary state $E_{tot} = K + U = -K$ with K the total kinetic energy, implying a negative heat capacity. As energy is non-additive in this case, the usual argument

that a negative heat capacity implies instability does not apply [24]. Nevertheless there is no truly stationary state for a self-gravitating system as the potential is unbounded from below and also non-confining, which imply that the entropy has at most a local maximum or even no maximum at all, as well discussed by Antonov [6, 11]. But model systems corresponding to real physical situations with the occurrence of a convex intruder in the entropy do exist, such as two-dimensional quasi-geostrophic flows [14] and wave-particle interaction in a plasma in the presence of two harmonics [15, 16]. In both cases heat capacity is negative in some energy interval. These, alongside self-gravitating systems and charged plasmas, are examples of long-range interacting systems, which are systems with interacting potentials decaying at long-distances as $1/r^\alpha$ with $\alpha < D$, D being the spatial dimension [17–22].

In order to understand and grasp the physics of many particles long-range interaction systems, some simplified models have been thoroughly studied in the literature, such as one- and two-dimensional self-gravitating systems and plasmas, the Hamiltonian mean field model, and the self-gravitating ring model (SGR) (see [22] and references therein). The SGR model was introduced by Sota and collaborators [23] and describes a system of N particles constrained to move on a circle and interacting by a gravitational potential, regularized at short distances by a (usually small) softening parameter ϵ in order to avoid the divergence of the potential at short distances. With a proper choice of units its Hamiltonian can be written as:

$$H = \sum_{i=1}^{N} \frac{p_i^2}{2} - \frac{1}{2N} \sum_{i,j=1}^{N} \frac{2\sqrt{\epsilon}}{\sqrt{1 - \cos(\theta_i - \theta_j) + \epsilon}}, \tag{2}$$

with θ_i being the position angle on the circle of particle i and p_i its conjugate (angular) momentum. Units have been chosen such that the minimum value of the energy is -1 irrespective of the value of ϵ. The factor $1/N$ in the potential energy term is known as the Kac factor, and can be introduced by a change of time units (as long as N remains finite), in order for the total energy to be extensive, although remaining non-additive. The analogous of a magnetization can be introduced here by its components:

$$M_x = \frac{1}{N} \sum_{i=1}^{N} \cos\theta_i, \qquad M_y = \frac{1}{N} \sum_{i=1}^{N} \sin\theta_i. \tag{3}$$

Many properties of the model were studied in previous works [26–31]. It has a phase-transition from a low energy ferromagnetic phase to a high energy homogeneous (non-magnetic) phase. The order of the transition depends on the value of the softening pa-

rameter. For smaller values of ϵ the transition is first order and becomes continuous for higher values of the parameter. The main goal of the present paper is to study the inequivalence of the microcanonical and canonical ensembles for the ring model from first principles, using both Monte Carlo and molecular dynamics simulations, and discuss its physical consequences. This will be an illustration of how ensemble equivalence occurs in a continuous Hamiltonian system, and will also allow, as we hope, an unequivocal interpretation of how different ensembles must be interpreted in the presence of long-range, i. e. non-tempered, interactions, and of the physical meaning of the Maxwell construction for those systems.

The structure of the paper is the following: in Section II we present our Monte Carlo and molecular dynamics results for the ring model. In Section III we discuss the implications of our results for the thermodynamics of systems with long-range interactions followed by a conclusion.

II. MICROCANONICAL AND CANONICAL ENSEMBLES FOR THE SELF-GRAVITATING RING MODEL

The entropy per particle and the caloric curve for the self-gravitating ring model with the Hamiltonian in Eq. (2) can be obtained with a very high accuracy using an iterative variational method [29] for maximizing the Gibbs entropy per particle:

$$s \equiv S/N = -\int \mathrm{d}p\, \mathrm{d}\theta\, f_1(p,\theta) \ln f_1(p,\theta), \tag{4}$$

where we set the Boltzmann constant equal to unity and $f_1(p,\theta)$ is the 1-particle distribution function. We used the fact that in the $N \to \infty$ limit particles are exactly uncorrelated [32]. In the remaining we chose the value $\epsilon = 10^{-2}$ as the system has a negative heat capacity for an energy interval and at the same time it allows faster molecular dynamics simulations. The results for the caloric curve and the entropy as a function of energy per particle e are shown in Fig. 2, where a region of negative heat capacity is clearly visible as well as the corresponding convex dip in the entropy function. Note that the variational method is solely based on entropy maximization on the space of one-particle distribution functions, and the results obtained are thus a direct consequence of the second law of thermodynamics. Microcanonical Monte Carlo results were obtained using the method described in Ref. [33], and are also shown on the Fig. 2, with a very good agreement with the variational method.

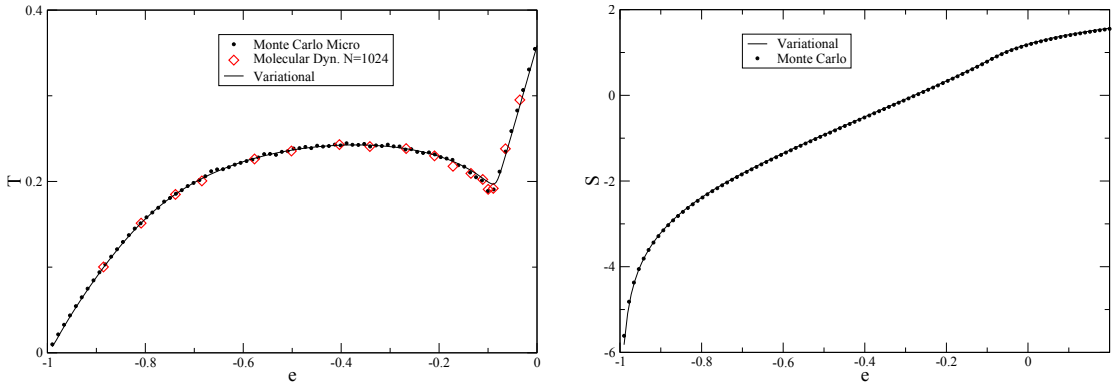

FIG. 2. Left Panel: caloric curve for the ring model with $\epsilon = 10^{-2}$ from the variational method in [29], microcanonical Monte Carlo simulations with $N = 1000$, and microcanonical molecular dynamics simulation with $N = 1024$ using a time step $\Delta t = 0.02$. Right Panel: entropy per particle as a function of energy.

One may ask whether the system can relax to an equilibrium state if its energy belongs to the region with a negative heat capacity. In order to answer that question we numerically solved the Hamiltonian equation of motion for the N particle system for many initial conditions for different energy values using a Graphics Processing Units parallel implementation [35] of a fourth-order simplectic integrator [34]. The system is initially prepared in a *waterbag* non-equilibrium state with a uniform distribution in the intervals $-p_0 < p < p_0$ and $-\theta_0 < \theta < \theta_0$, with the constants p_0 and θ_0 chosen for the system to have the required energy. Since the relaxation time to reach equilibrium is typically very long in long-range interacting systems, and scales with N for non-homogeneous or N^2 for homogeneous states [31, 37, 38], very long computer runs are required. The left panel of Fig. 3 shows the time evolution of the total kinetic K and potential V energies per particle for a homogeneous waterbag non-equilibrium initial state with $\theta_0 = \pi$ and total energy per particle $e = -0.135$. The total simulation time for this case is roughly 12 hours on a NVIDIA GTX 690 GPU. In order to measure the distance to equilibrium we use the kurtosis of the momentum distribution, i. e. the fourth reduced statistical moment of p given by $\mathcal{K} = \langle p^4 \rangle / \langle p^2 \rangle^2$. Its value for any Gaussian distribution is given by $\mathcal{K} = 3$. The right panel of Fig. 3 shows the kurtosis of the momentum distribution, where we see that the system reaches equilibrium at $t \approx 2 \times 10^5$. Data obtained from such simulation is presented in the microcanonical caloric curve in Fig. 2, showing a very good agreement with both microcanonical Monte Carlo and

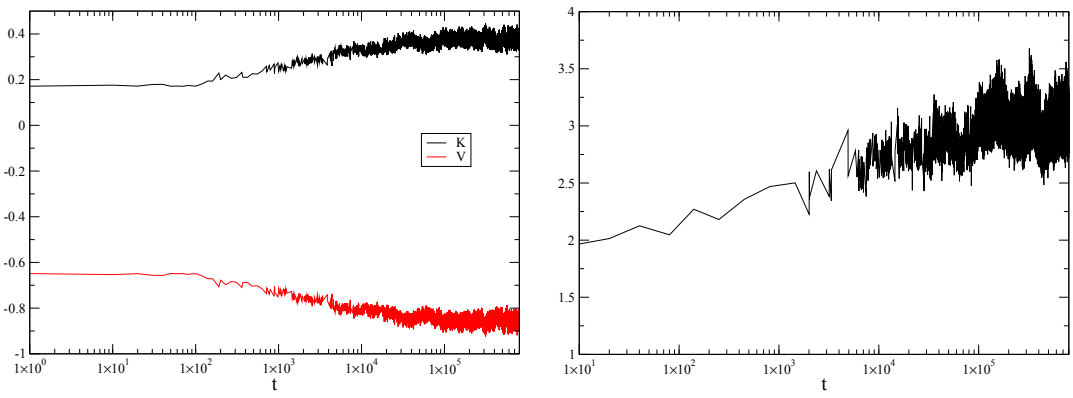

FIG. 3. Left Panel: Kinetic K and potential V energies per particle as a function of time for a homogeneous waterbag initial state with total energy per particle $e = -0.135$ which correspond to an equilibrium state with a negative heat capacity, simulation time step $\Delta t = 0.02$ with a relative error in the energy of order 10^{-6}. Right Panel: Kurtosis as a function of time.

variational methods. Thus, at least for the present model, equilibrium states with a negative heat capacity are accessible by relaxation from non-equilibrium states.

The next point to consider is to determine the caloric curve in the canonical ensemble. Canonical Monte Carlo results are show in the left panel of Fig. 4, alongside with points obtained from the minimization of the free energy. The latter was obtained using the usual relation $F = E - TS$ with the entropy computed from Eq. (4) by writing

$$f_1(p, \theta) = \sqrt{\beta/2\pi}\, e^{-\beta p^2/2} \rho(\theta) \tag{5}$$

and the (normalized) spatial distribution $\rho(\theta)$ given a histogram of the particle positions from the microcanonical Monte Carlo simulation. The free energy F as a function of temperature can also be obtained by the Legendre transform of the entropy as obtained using the variation method, and is shown in the right panel of Fig. 4, where a van der Waals loop is clearly visible. Both results from canonical Monte Carlo and free energy minimization are in quite good agreement except for a few points corresponding to metastable states close to $e = -0.55$. Such states, being local minima of the free energy, trap the Monte Carlo evolution for a very large number of steps and are known to cause numerical difficulties. The relatively small number of particles $N = 300$ used in the simulation is for limiting the effects of such metastable states.

Now if the system, in a microcanonical equilibrium state with a negative heat capacity, is

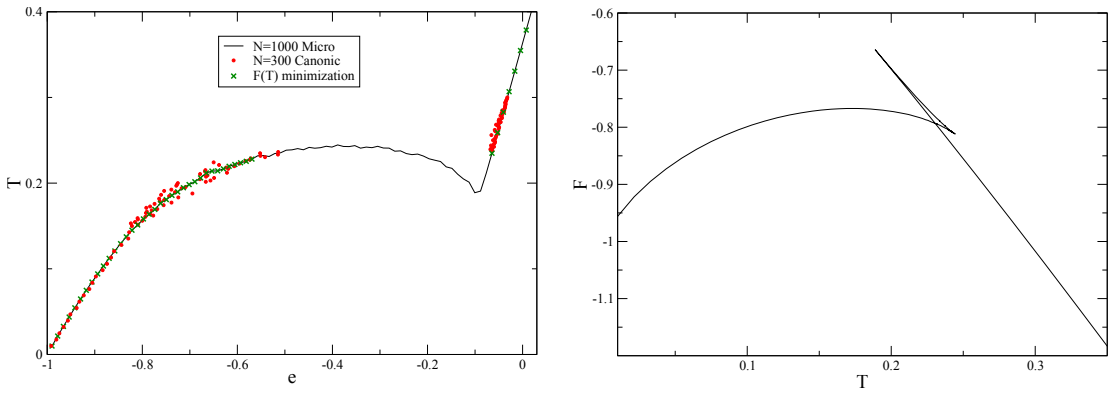

FIG. 4. Left Panel: Caloric curve for the ring model with $\epsilon = 10^{-2}$ from microcanonical and canonical Monte Carlo simulations with $N = 1000$ and $N = 300$, respectively. The crosses correspond to the minimization of the Helmholtz free energy. Right Panel: Helmholtz free energy obtained from the Legendre transform of the entropy.

put in contact with a thermal bath at the same temperature, it becomes unstable and evolves to the canonical equilibrium state that minimizes the free energy, for the same temperature of the initial state. We illustrate this from first principles by performing a molecular dynamics simulation of both system and thermal bath. Following the same approach as in Ref. [36], the bath is given by a Hamiltonian system with a short-range interaction formed by M rotors with Hamiltonian:

$$H_{bath} = \sum_{i=N+1}^{N+M} \frac{p_i^2}{2} + \sigma \sum_{i=N+1}^{N+M} \left[1 - \cos(\theta_i - \theta_{i+1})\right], \tag{6}$$

where θ_i and p_i the coordinates and the momenta of particle i, with $\theta_{N+M+1} \equiv \theta_{N+1}$ and σ the interaction strength among first neighbors. The number of particles in the bath is chosen such that $M \gg N$ to guarantee that the main system only causes minor disturbances in the bath. The SGR model and the bath are coupled by the interaction potential:

$$V_{int} = \lambda \sum_{i=1}^{L} \left[1 - \cos(\theta_i - \theta_{i+N})\right], \tag{7}$$

with λ the coupling parameter and L chosen typically as a fraction of N. The total Hamiltonian is then the sum of the Hamiltonian in Eq. (2), H_{bath} and V_{int}. The choice of the parameters requires some experimentation, and the values used here are $N = 512$, $M = 204\,800$, $L = 16$, $\sigma = 5.0$ and $\lambda = 1.0$. The left panel in Fig. 5 shows the time evolution to equilibrium of an isolated ring model waterbag initial state with energy $e = -0.2$, which lies inside

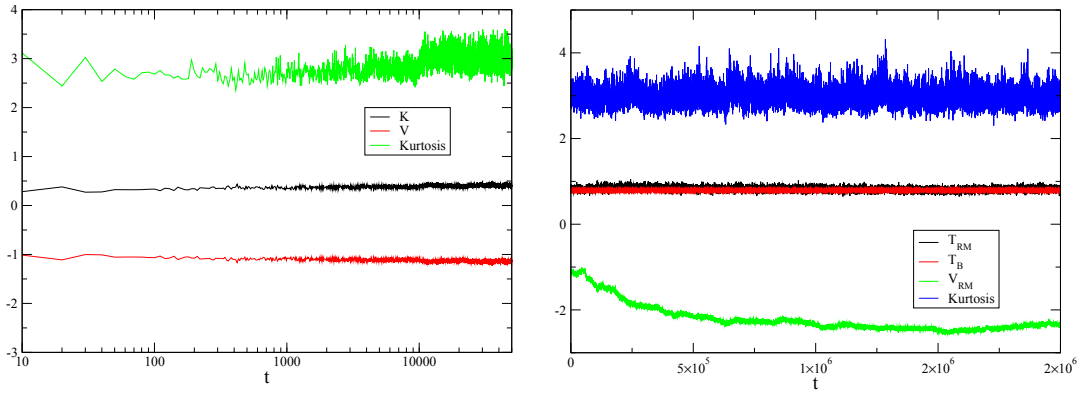

FIG. 5. Left Panel: Evolution to thermodynamic equilibrium of a waterbag initial state with energy per particle $e = -0.2$. Right Panel: Time evolution of the same microcanonical equilibrium state at energy per particle $e = -0.2$ of the left panel when in contact with a heat bath ate the same temperature. The simulation parameters are $\Delta t = 0.02$, $t_f = 2 \times 10^6$.

the negative heat capacity energy interval. The resulting microcanonical equilibrium state is then coupled to the thermal bath. The time evolution of temperature as given by twice the kinetic energy, of the kurtosis of the velocity distribution for the main system, and the interaction energy between the system and the bath are show in the right panel of the same figure. The ring model starts from the now unstable initial state and evolves to a canonical equilibrium while the temperature remains constant, up to small fluctuations. The kurtosis remains always close to the equilibrium value, indicating that the momentum distribution function remains a Gaussian during the whole time evolution. The spatial distribution function changes until the final state corresponds to the minimum of the free energy. This can be verified from the final canonical equilibrium state as shown in Fig. 6, the temperature from Fig. 5 and the plot of the free energy in Fig. 4.

III. DISCUSSION AND CONCLUSIONS

From the results above we see that in the canonical ensemble, i. e. for a system coupled to a large energy reservoir, the whole energy interval corresponding to the Maxwell construction does not exist in the canonical ensemble. All states with energy in the interval (E_A, E_B) in Fig. 1 cannot be realized physically as an equilibrium state. If the temperature is slowly raised starting from $T(E_A)$, the temperature at energy E_A, the energy jumps discontinuously

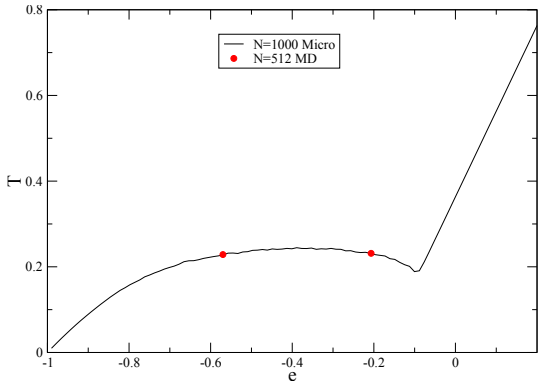

FIG. 6. Initial ($e = -0.2$) and final ($e \approx -0.57$) states for a microcanonical stable state in the negative heat capacity region after turning on the coupling to a heat bath. the ring model system has $N = 512$ particles and the bath $N_b = 204\,800$ particles. The simulation parameters are $\Delta t = 0.02$, $t_f = 2 \times 10^6$.

from E_A to E_B. If the system is in a state with energy in this interval, it will absorb from or give energy to the bath until it reaches a stable canonical equilibrium that minimizes the free energy, as expected [13] and as was illustrated from a direct numerical simulation.

It is common when computing statistical mechanics properties of a short-range interacting system to rely on some approximation that results in a van der Waals loop, e. g. using a mean-field approximation. In this case replacing the convex dip in the entropy function by a flat line according to the Maxwell construction prescription is fully justified, as the entropy of the original system is additive, although this property is usually not satisfied in a mean-field approximation. On the other hand, if the system has long-range interactions, or equivalently non tempered and of not satisfying the condition of van Hove's theorem, then the convex dip may not disappear in the thermodynamic limit. Using the Maxwell construction in this case is plainly wrong as it leads to physically non realizable states. In this case, the correct prescription is to take the whole region corresponding to a negative heat capacity (energies in the interval (E_A, E_B) in Fig. 1) as non physical. This is equivalent to discard van der Waals loops when present in the free energy. A purely thermodynamic description of long-range interacting systems remains possible along the lines discussed in Refs. [39, 40].

IV. ACKNOWLEDGMENTS

The authors would like to thank S. R. Salinas and V. B. Henriques for fruitful discussions. TMRF was partially financed by CNPq (Brazil) and CHS was financed by CAPES (Brazil).

---

[1] J. W. Gibbs, *Elementary Principles in Statistical Mechanics with Special Reference to the Rational Foundation of Thermodynamics*, Yale University Press (Yale,1902). Reprinted by Dover (New York, 1960).

[2] H. Inaba, Eur. Phys. J. H **40**, 489 (2015).

[3] J. T. Lewis, C.-E. Pfister and W. G. Sullivan, J. Stat. Phys. **77**, 397 (1994).

[4] R. S. Ellis, K. Haven, B. Turkington, J. Stat. Phys. **101** , 999 (2000).

[5] D. Ruelle, *Statistical Mechanics - Rigourous Results*, World Scientific - Imperial College Press (London, 1999).

[6] J. B. Binney and S. Tremaine, *Galactic Dynamics*, 2nd Ed, Princeton Univ. Press (Princeton, 2008).

[7] L. van Hove, Physica **15**, 951 (1949).

[8] D. Wales and J. P. K. Doye, J. Chem. Phys. **103** 3061 (1995).

[9] R. M. Lynden-Bell and D. J. Wales, J. Chem. Phys. **101** 1460 (1994).

[10] D. H. E. Gross, *Microcanonical Thermodynamics - Phase Transisitions in "Small" Systems* World Scientific (Singapore, 2001).

[11] V. A. Antonov *Dynamics and Star Clusters*, in: J. Goodman and P. Hut (eds.), pp. 525-540 (1985) (International Astronomical Union).

[12] I. Ispolatov, E. G. D. Cohen, Physica A **295**, 475 (2001).

[13] H. Touchette, R. S. Ellis and B. Turkington, Physica A **340**, 138 (2004).

[14] B. E. Turkington, *Statistocal Mechabics of two-dimensional quasi-geostrophic flows*, in *Lon-Range Interacting Systems*, Les Houches 2008, Session XC, T. Dauxois, S. Ruffo and L. F. Cugliandolo Eds, Oxford Univ. Press (Oxford, 2010).

[15] Y. Elskens and D. Escande, *Microscopic Dynamics of Plasmas and Chaos*, Intitute of Physics (Bristoli, 2003).

[16] T. N. Teles, D. Fanelli and S. Ruffo, Phys. Rev. E **89**, 050101(R) (2014).

[17] *Dynamics and Thermodynamics of Systems with Long-Range Interactions*, T. Dauxois, S. Ruffo, E. Arimondo and M. Wilkens Eds. (Springer, Berlin, 2002).

[18] *Dynamics and Thermodynamics of Systems with Long-Range Interactions: Theory and Experiments*, A. Campa, A. Giansanti, G. Morigi and F. S. Labini (Eds.), AIP Conf. Proceedings Vol. 970 (2008).

[19] *Long-Range Interacting Systems, Les Houches 2008, Session XC*, T. Dauxois, S. Ruffo and L. F. Cugliandolo Eds. (Oxford Univ. Press, Oxford, 2010).

[20] A. Campa, T. Dauxois, D. Fanelli and S. Ruffo, *Physics of Long-Range Interacting Systems*, Oxford University Press (Oxford, 2014).

[21] A. Campa, T. Dauxois, and S. Ruffo, Phys. Rep. **480** (2009) 57.

[22] Y. Levin, R. Pakter, F. B. Rizzato, T. N. Teles and F. P. C. Benetti, Phys. Rep. **535**, 1 (2014).

[23] Y. Sota, O. Iguchi, M. Morikawa, T. Tatekawa and K. I. Maeda, Phys. Rev. E **64**, 056133 (2001).

[24] W. Thirring, Z. Phys. **235**, 339 (1970).

[25] A. Campa, T. Dauxois and S. Ruffo, Phys. Rep. **480**, 57 (2009).

[26] T. M. Rocha Filho, M. A. Amato, B. A. Mello and A. Figueiredo, Phys. Rev. E **84**, 041121 (2011).

[27] L. Casetti and C. Nardini, J. Stat. Mech. P05006 (2010).

[28] B. Monechi and L. Casetti, Phys. Rev. E **86**, 041136 (2012).

[29] T. Tatekawa, F. Bouchet, T. Dauxois and S. Ruffo, Phys. Rev. E **71**, 056111 (2005).

[30] C. Nardini and L. Casetti, Phys. Rev. E **80**, 060103(R) (2009).

[31] T. M. Rocha Filho, M. A. Amato, A. E. Santana, A. Figueiredo and J. R. Steiner Phys. Rev. E **89**, 032116 (2014).

[32] P.-H. Chavanis, Physica A **361**, 55 (2006).

[33] J. Ray, Phys. Rev. A **44**, 4061, (1991).

[34] H. Yoshida, Phys. Lett. A **150**, 262 (1990).

[35] T. M. Rocha Filho, Comp. Phys. Comm. **185**, 1364 (2014).

[36] T. M. Rocha Filho, A. Figueiredo and M. A. Amato, Phys. Rev. Lett. **95**, 190601 (2005)

[37] T. M. Rocha Filho, A. E. Santana, M. A. Amato and A. Figueiredo, Phys. Rev. E **90**, 032133 (2014).

[38] C. R. Lourenço and T. M. Rocha Filho, Phys. Rev. E **92**, 012117 (2015).

[39] I. Latella and P. Pérez-Madrid, Phys. Rev. E **88**, 042135 (2013).

[40] I. Latella, A. Pérez-Madrid, A. Campa, L. Casetti and S. Ruffo, Phys. Rev. Lett. **114**, 230601 (2015).